Cement and Concrete Research 41 (2011) 987–992

Contents lists available at ScienceDirect

Cement and Concrete Research

journal homepage: http://ees.elsevier.com/CEMCON/default.asp

# Why alite stops hydrating below 80% relative humidity

Robert J. Flatt [a], George W. Scherer [b,*], Jeffrey W. Bullard [c]

[a] Sika Technology AG, Zürich, Switzerland
[b] Princeton University, Eng. Quad. E-319, Princeton NJ 08544, USA
[c] National Institute of Standards and Technology, Gaithersburg MD, USA

ARTICLE INFO

*Article history:*
Received 15 July 2010
Accepted 6 June 2011

*Keywords:*
A. Humidity
A. Hydration
A. Reaction

ABSTRACT

It has been observed that the hydration of cement paste stops when the relative humidity drops below about 80%. A thermodynamic analysis shows that the capillary pressure exerted at that RH shifts the solubility of tricalcium silicate, so that it is in equilibrium with water. This is a reflection of the chemical shrinkage in this system: according to Le Chatelier's principle, since the volume of the products is less than that of the reactants, a negative (capillary) pressure opposes the reaction.



## 1. Introduction

Cement hydration continues to have an intriguing character, surrounded as it is by a number of intensively debated questions. Among the unresolved issues is the reason why hydration of a cement paste stops at a relative humidity of about RH = 0.8, even though the system still contains a significant amount of water [1–5]. For example, Jensen et al. [6] report that triclinic $C_3S$[1] has a degree of hydration of 36% after 90 days at RH = 0.98, but a degree of hydration of only 2% after 90 days when the RH is lowered to 0.85.

This communication shows that a critical relative humidity, below which hydration should stop, can be defined from a relatively simple thermodynamic treatment. Similar analyses have been attempted in the past. Jensen [7] calculated the vapor pressure at which hydration would stop in the absence of condensed water. He found that extremely low RH was required to establish equilibrium between clinker and various mineral phases (*e.g.*, RH<0.01 for equilibrium between clinker and tobermorite). In the present work, we show that the decrease in water activity needed to arrest hydration results from the negative capillary pressure in the pore liquid at RH ≤ 0.8.

## 2. Theory

The basic idea is that the system stops hydrating if $C_3S$, C–S–H and CH are all simultaneously in equilibrium. This does not happen when excess water is available; however, as relative humidity decreases, the reduction in water activity can allow this equilibrium to be established.

The results of this analysis are particularly sensitive to the selection of the thermodynamic data. This is especially true for $C_3S$ solubility. Indeed, there are different hypotheses to account for the rapid deceleration of $C_3S$ reaction after contact with water. One suggestion is that dissolution involves a step of surface hydroxylation, so that it is the solubility product of this layer rather than that of bulk $C_3S$ that should be used [8–10]. Recent work suggests that the solubility of this layer is 17 orders of magnitude lower than the one obtained from bulk thermodynamics [11,12], and there still is not universal agreement on the value or meaning of alite solubility product, so much caution is warranted when interpreting the results presented here.

In this communication, we use the same data as Bullard and Flatt [13] who found those data to lead to a good prediction of $C_3S$ hydration kinetics using HydratiCA, a kinetic cellular automaton model [14]. In particular, they correctly capture the kinetics of heat release by $C_3S$ hydration as well as the evolution of ionic concentrations in solution [13].

## 3. Reactions

The dissolution reaction for $C_3S$ is assumed to be [13]:

$$Ca_3SiO_5 + 3H_2O \rightleftharpoons 3Ca^{2+} + H_2SiO_4^{2-} + 4OH^-. \quad (1)$$

C–S–H is modeled as a mixture of two phases denoted $CSH_4$=$Ca(OH)_2 \cdot SiO_2 \cdot 3H_2O$ and $C_2SH_7$=$2Ca(OH)_2 \cdot SiO_2 \cdot 5H_2O$ with Ca/Si ratios of 1 and 2, respectively [13,14]. For these, the dissolution reactions are:

$$Ca(OH)_2 \cdot SiO_2 \cdot 3H_2O \rightleftharpoons Ca^{2+} + H_2SiO_4^{2-} + 3H_2O \quad (2)$$

* Corresponding author. Tel.: +1 609 258 5680.
*E-mail address:* scherer@princeton.edu (G.W. Scherer).

[1] We use conventional cement chemistry notation, *e.g.* C = CaO, S = $SiO_2$, H = $H_2O$.

0008-8846/$ – see front matter © 2011 Elsevier Ltd. All rights reserved.
doi:10.1016/j.cemconres.2011.06.001

$$2Ca(OH)_2 \cdot SiO_2 \cdot 5H_2O \rightleftharpoons 2Ca^{2+} + H_2SiO_4^{2-} + 2OH^- + 5H_2O. \quad (3)$$

For calcium hydroxide we have:

$$Ca(OH)_2 \rightleftharpoons Ca^{2+} + 2OH^-. \quad (4)$$

Combining reactions (1), (2), and (4), we find the equilibrium between $C_3S$ and $CSH_4$:

$$C_3S + 6H \rightleftharpoons CSH_4 + 2CH. \quad (5)$$

We can also combine reactions (1) and (4) with (3) to find the equilibrium between $C_3S$ and $C_2SH_7$:

$$C_3S + 8H \rightleftharpoons C_2SH_7 + CH. \quad (6)$$

## 4. Equilibrium constants

The chemical potential of each component $i$ in the system is given by

$$\mu_i = \mu_i^0 + \overline{V}_i(P - P_0) + R_gT\ ln(a_i) \quad (7)$$

where $\mu_i^0$ is the standard chemical potential of the pure component at atmospheric pressure, $P_0$, $\overline{V}_i$ is the partial molar volume, $R_g$ is the ideal gas constant, $T$ is the temperature, and $a_i$ is the activity of component $i$. For a reaction of the type,

$$aA + bB + \ldots \leftrightarrow eE + fF + \ldots \quad (8)$$

the chemical potential change is

$$\Delta\mu = (e\mu_E + f\mu_F + \ldots) - (a\mu_A + b\mu_B + \ldots). \quad (9)$$

Using Eq. (7) to represent each component in Eq. (9), we can write

$$\Delta\mu(P) = \Delta\overline{V}(P - P_0) + R_gT\ ln\left(\frac{Q}{K}\right) \quad (10)$$

where the equilibrium constant (or, solubility product), $K$, is defined by

$$\Delta\mu_0(P_0) = \left(e\mu_E^0 + f\mu_F^0 + \ldots\right) - \left(a\mu_A^0 + b\mu_B^0 + \ldots\right) = -R_gT\,ln(K) \quad (11)$$

and the activity product, $Q$, is

$$Q = \frac{a_E^e a_F^f \ldots}{a_A^a a_B^b \ldots}. \quad (12)$$

The molar volume change is

$$\Delta\overline{V} = (e\overline{V}_E + f\overline{V}_F + \ldots) - (a\overline{V}_A + b\overline{V}_B + \ldots). \quad (13)$$

The reaction will proceed spontaneously to the right if $\Delta\mu<0$; at atmospheric pressure, this happens when $Q<K$. At equilibrium, $\Delta\mu=0$; at atmospheric pressure, this condition means that the activity product, $Q$, is equal to $K$. For Eq. (5), for example,

$$K_{C_3S \leftrightarrow CSH_4} = \frac{a_{CSH_4}(a_{CH})^2}{a_{C_3S}(a_H)^6} = \frac{1}{(a_H)^6} \quad (14)$$

where the second equality follows from the fact that the activities of the pure solids are equal to unity. By using Eq. (11) to write out $K$ for reactions (1), (2), and (4), one can directly verify that

$$K_{C3S \leftrightarrow CSH_4} = \frac{K_{C3S}}{K_{CSH_4}(K_{CH})^2}. \quad (15)$$

Similarly, for Eq. (6) we find

$$K_{C3S \leftrightarrow C_2SH_7} = \frac{1}{(a_H)^8} = \frac{K_{C3S}}{K_{C_2SH_7}K_{CH}}. \quad (16)$$

The equilibrium constants for the reactions cited above at atmospheric pressure, $P_0$, are given in Table 1. The analysis used here depends significantly on these values, so a few comments are warranted about our confidence in them. First, the value for the solubility of CH in Eq. (20) in the table is well-established in thermodynamic databases [15] and validated by careful experimental observations [16]. Second, for the two types of C–S–H used here, there is some experimental evidence that C–S–H is a binary solid solution with a narrow miscibility gap and two end members having molar Ca/Si ratios of about 1.2 and 2.0, respectively [17]. We have adopted similar stoichiometries for the end members here, and we have estimated their solubilities from the published solubility curve in Ref. [17]. These solubilities are also consistent with the low-Ca and high-Ca portions of the solubility curve B proposed by Jennings [18], and from the latter we estimate the uncertainty in the exponents of Eqs. (18) and (19) in the table as $\pm 0.3$. Finally, the solubility product for $C_3S$ is much more controversial and poorly defined than for either CH or C–S–H. The value calculated using tabulated free energies of formation is about 3 [11], but this value is extremely large compared to observed pore solution compositions during the induction period of hydration. The most recent research in environmental geochemistry suggests that the mechanism of the dissolution of silicate minerals changes from etch pit unwinding at high driving forces to crystallographic step edge retreat at moderate driving forces, so that the dissolution rate varies in a highly nonlinear way as a function of undersaturation [19]. The consequence for these minerals is that their dissolution rate becomes exceedingly slow when the undersaturation is still moderately large. This concept has recently been applied to analyze the dissolution of alite [20] and compare it with measured dissolution rates of alite as a function of solution composition at early ages [21]. The consequence is that alite dissolution rates decrease by a factor of about 100 from their initial values when the activity product in Eq. (17) in the table is still 37 orders of magnitude lower than the equilibrium value. Nonat et al. have measured $C_3S$ dissolution rates in stirred suspensions so dilute that neither C–S–H nor CH should precipitate, and have found that dissolution essentially stops when the activity product is about $10^{-17}$ (A. Nonat, personal communication). Values very similar to this, between $10^{-17}$ and $10^{-17.1}$ have been used in kinetic cellular automaton simulations of hydration that are consistent with experimental observations of hydration rates and evolution of solution composition [13,22]. In light of the accumulated evidence just described, we use a value for the solubility product of alite between $10^{-17}$ and $10^{-18}$ as the best estimate currently available.

**Table 1**
Equilibrium constants at atmospheric pressure, $P_0$ [13].

| | | |
|---|---|---|
| $K_{C3S} = \frac{\left(a_{Ca^{2+}}\right)^3 a_{H_2SiO_4^{2-}} (a_{OH^-})^4}{(a_H)^3}$ | $K_{C3S}^{P_0} \approx 10^{-18} - 10^{-17}$ | (17) |
| $K_{CSH_4} = a_{Ca^{2+}} a_{H_2SiO_4^{2-}} (a_H)^3$ | $K_{CSH_4}^{P_0} = 10^{-7.52}$ | (18) |
| $K_{C_2SH7} = (a_{Ca^{2+}})^2 a_{H_2SiO_4^{2-}} (a_{OH^-})^2 (a_H)^5$ | $K_{C_2SH7}^{P_0} = 10^{-12.96}$ | (19) |
| $K_{CH} = a_{Ca^{2+}} (a_{OH^-})^2$ | $K_{CH}^{P_0} = 10^{-5.2}$ | (20) |
| $K_{C3S \leftrightarrow CSH_4} = \frac{1}{(a_H)^6}$ | $K_{C3S \leftrightarrow CSH_4}^{P_0} = \frac{K_{C3S}^{P_0}}{K_{CSH_4}^{P_0} \left(K_{CH}^{P_0}\right)^2} = 10^{0.92}$ | (21) |
| $K_{C3S \leftrightarrow C_2SH_7} = \frac{1}{(a_H)^8}$ | $K_{C3S \leftrightarrow C_2SH_7}^{P_0} = \frac{K_{C3S}^{P_0}}{K_{C_2SH_7}^{P_0} K_{CH}^{P_0}} = 10^{1.16}$ | (22) |

## 5. Role of capillary pressure

Experience indicates that $C_3S$ will dissolve completely in water (that is, Eq. (1) will proceed all the way to the right), so no equilibrium will be achieved, unless the RH is below about 0.8. Given the numerical values for the equilibrium constants in Table 1, Eqs. (21) and (22) indicate that the reaction will proceed until the activity of water is reduced to 0.70 and 0.72, respectively. This prediction is in reasonable agreement with the experimentally observed value of about 0.8 [4], but much of the apparent discrepancy can be accounted for quantitatively by considering the effect of capillary pressure on the solubilities of $C_3S$, C–S–H, and CH. That is, in a partially saturated system, the capillary pressure caused by curvature of the liquid–vapor meniscus in the pore space causes a perceptible shift in the net equilibrium state. Since the hydration of $C_3S$ results in chemical shrinkage [23], negative capillary pressure inhibits dissolution.

At pressures other than $P_0$, the condition for equilibrium is found by setting $\Delta\mu = 0$ in Eq. (10):

$$Q = K \exp\left[-\frac{\Delta\overline{V}(P-P_0)}{R_gT}\right] \tag{23}$$

For the net hydration reaction given by Eq. (5),

$$\Delta\overline{V} = \overline{V}_{CSH_4} + 2\overline{V}_{CH} - \overline{V}_{C3S} - 6\ \overline{V}_H \equiv \Delta\overline{V}_I \tag{24}$$

so Eqs. (14) and (15) are replaced by

$$\frac{1}{(a_H)^6} = \frac{K_{C3S}}{K_{CSH_4}(K_{CH})^2} \exp\left[-\frac{\Delta\overline{V}_I(P-P_0)}{R_gT}\right] \tag{25}$$

or, using Eq. (15),

$$a_H = K_{C3S\leftrightarrow CSH_4}^{-1/6} \exp\left[\frac{\Delta\overline{V}_I(P-P_0)}{6R_gT}\right]. \tag{26}$$

Similarly, for the net hydration reaction in Eq. (6),

$$\Delta\overline{V} = \overline{V}_{C_2SH_7} + \overline{V}_{CH} - \overline{V}_{C3S} - 8\ \overline{V}_H \equiv \Delta\overline{V}_{II} \tag{27}$$

so Eq. (16) is replaced by

$$\frac{1}{(a_H)^8} = \frac{K_{C3S}}{K_{C_2SH_7}K_{CH}} \exp\left[-\frac{\Delta\overline{V}_{II}(P-P_0)}{R_gT}\right] \tag{28}$$

or

$$a_H = K_{C3S\leftrightarrow C_2SH_7}^{-1/8} \exp\left[\frac{\Delta\overline{V}_{II}(P-P_0)}{8R_gT}\right]. \tag{29}$$

To make use of these results, we need an expression relating the pressure to the RH, which we now obtain.

The chemical potential of water vapor is

$$\mu_{H,V} = \mu_{H,0} + R_gT\ ln\left(\frac{p_v}{p_0}\right) \equiv \mu_{H,0} + R_gT\ ln\,(\mathrm{RH}) \tag{30}$$

where $p_v$ is the vapor pressure of the water, $p_0(T)$ is the saturation vapor pressure at temperature $T$, and $\mathrm{RH} = p_v/p_0$ is the relative humidity. The chemical potential of the liquid is

$$\mu_{H,L} = \mu_{H,0} + \overline{V}_H(P-P_0) + R_gT\ ln(a_H). \tag{31}$$

For pure water, $a_H = 1$, so the pressure in the liquid is related to the RH by the Kelvin equation,

$$P = P_0 + \frac{R_gT}{\overline{V}_H} \ln(\mathrm{RH}). \tag{32}$$

When the solution is in equilibrium with the vapor, $\mu_{H,V} = \mu_{H,L}$, so Eqs. (30) and (31) require

$$a_H = \mathrm{RH} \exp\left[-\frac{\overline{V}_H(P-P_0)}{R_gT}\right] \tag{33}$$

so

$$\exp\left[\frac{(P-P_0)}{R_gT}\right] = \left(\frac{\mathrm{RH}}{a_H}\right)^{1/\overline{V}_H}. \tag{34}$$

These relations indicate that the RH can be reduced by a high solute content ($a_H < 1$) or a negative (capillary) pressure in the liquid. In the present case, the solubilities of the products are low (the solute concentrations are in the mmol/L range [24]), so $a_H \approx 1$ by Raoult's Law. Therefore, a low RH can only result from a large capillary pressure.

Now we can relate the relative humidity to the conditions for equilibrium. If we use Eq. (34) in Eq. (26), we find

$$a_H = K_{C3S\leftrightarrow CSH_4}^{-1/6} \left(\left(\frac{\mathrm{RH}}{a_H}\right)^{1/\overline{V}_H}\right)^{\Delta V_I/6} \tag{35}$$

or

$$\mathrm{RH} = \left(K_{C3S\leftrightarrow CSH_4}\right)^{\overline{V}_H/\Delta\overline{V}_I} a_H^{6\overline{V}_H/\Delta\overline{V}_I+1} \approx \left(K_{C3S\leftrightarrow CSH_4}\right)^{\overline{V}_H/\Delta\overline{V}_I}. \tag{36}$$

The approximation in Eq. (36) is valid in the present case because, as already shown, $a_H \approx 1$. Thus, reaction (5) will come to equilibrium (*i.e.*, dissolution of $C_3S$ will stop) at the RH given by Eq. (36). Similarly, from Eqs. (34) and (29), we find that Eq. (6) will come to equilibrium at the RH given by

$$\mathrm{RH} = \left(K_{C3S\leftrightarrow C_2SH_7}\right)^{\overline{V}_H/\Delta\overline{V}_{II}} a_H^{8\overline{V}_H/\Delta\overline{V}_{II}+1} \approx \left(K_{C3S\leftrightarrow C_2SH_7}\right)^{\overline{V}_H/\Delta\overline{V}_{II}}. \tag{37}$$

## 6. State of stress in the solid

In the preceding analysis, we have assumed that the solid (clinker) is subjected to the same negative pressure as the pore liquid. In fact, the solid is in a nonhydrostatic state of stress with a mean stress (*i.e.*, trace of the stress tensor) that is compressive. This is evident from a force balance, since the suction in the liquid must be balanced by compression in the solid; this compressive stress is what drives autogenous shrinkage, and what makes the body contract as it dries. At the surface of a particle of clinker, the normal stress, $\sigma_n$, is balanced by the pressure in the liquid ($\sigma_n = -P$), but the other stress components are different and combine to give a negative mean stress. Sekerka and Cahn [25] have shown that when a solid is in contact with its melt at its surface, but has a nonhydrostatic state of stress internally, then the solid is unstable with respect to a hydrostatically stressed solid at a pressure equal to that of the fluid. However, the shift in the equilibrium is very small; indeed, it is orders of magnitude smaller than the shift that would be predicted on the basis of the mean stress in the solid (see details in Appendix 1). A similar conclusion was reached by Paterson by a more elaborate procedure [26]. This means that our assumption that the pressure is the same in the clinker and the pore liquid will not lead to a significant error. That

is, the equilibrium is determined primarily by the pressure at the solid/liquid interface; the other stress components contribute only a small amount of elastic strain energy that has a negligible influence on the equilibrium. Recent experiments by Bisschop [27] confirm that nonhydrostatic stress has a negligible effect on the hydration rate of clinker in water at atmospheric pressure. Nevertheless, when we predict that the dissolution will stop, there is still a very small driving force for the reaction to continue, so as to eliminate the nonhydrostatic stress in the clinker.

## 7. Evaluation

According to Eqs. (36) and (37), the critical RH at which hydration will stop can be estimated if the molar volumes of the C–S–H phases are known. Since the densities of our hypothetical phases are not known, we will use the molar volumes of tobermorite (47.2 $cm^3$/mole [28]), jennite (76.2 $cm^3$/mole [29]), and C–S–H with C/S = 1.7 as reported by Jennings [30] (88.5 $cm^3$/mole). For the minerals, we normalize the volume by the number of Si in the formula unit; for the C–S–H, we use the density corresponding to a sample dried at 11% RH (to exclude evaporable water). As indicated in Fig. 1, the values fall very close to a straight line described by

$$V_M \approx 15.15 + 42.16\ (\mathrm{Ca/Si}). \tag{38}$$

From the fit, we estimate that $\overline{V}_{CSH_4} \approx 57.3$ $cm^3$/mole and $\overline{V}_{C_2SH_7} \approx 99.5$ $cm^3$/mole. Given $\overline{V}_{CH} = 33.1$ $cm^3$/mole, $\overline{V}_{C3S} = 73.2$ $cm^3$/mole, and $\overline{V}_H = 18.0$ $cm^3$/mole, we find $\Delta\overline{V}_I \approx -57.7$ $cm^3$/mole and $\Delta\overline{V}_{II} \approx -84.6$ $cm^3$/mole. With these values, the exponents in Eqs. (36) and (37) are found to be $\overline{V}_H / \Delta\overline{V}_I \approx -0.31$ and $\overline{V}_H / \Delta\overline{V}_{II} \approx -0.21$, respectively. For equilibrium to occur at RH ≈ 0.8, the equilibrium constants would have to be $K_{C3S \leftrightarrow CSH_4} \approx 2.05$ and $K_{C3S \leftrightarrow C_2SH7} \approx 2.89$; that is, $\log_{10} K_{C3S} \approx -17.65 \pm 0.05$ for both. This latter value for the solubility product of $C_3S$ agrees well with our best-estimate range of values already discussed and shown in Table 1. In fact, because a $K_{C3S}$ in this range has now separately been shown to explain the critical RH below which hydration of alite stops, our confidence in this range for the solubility is strengthened. On the other hand, if future studies show that $K_{C3S}$ is larger than this, then we should expect the hydration of $C_3S$ to slow down at RH < 0.8, but not necessarily to stop.

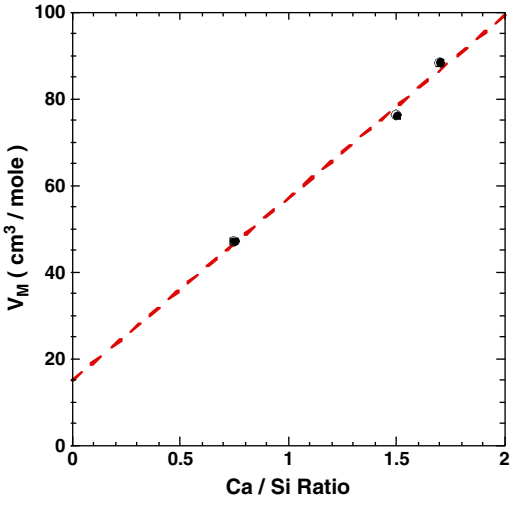


**Fig. 1.** Molar volume of tobermorite (Ca/Si = 0.75) [28], jennite (Ca/Si = 1.5) [29], and C–S–H (Ca/Si = 1.7) [30]. Dashed line is a least-squares fit of the reported values. Cited sources did not provide uncertainty estimates for the report values.

A water activity of 0.8 corresponds to a capillary pressure of about -30 MPa. The pressure is related by the Laplace equation to the radius of the meniscus, $r_m$, and the radius of the largest filled pore, $r_p$, by

$$P - P_0 = \frac{2\gamma_{LV}}{r_m} = -\frac{2\gamma_{LV}\ cos(\theta)}{r_p - \delta} \tag{39}$$

where $\gamma_{LV} = 0.072$ J/$m^2$ is the surface energy of water (which is barely affected by the solute), $\theta$ is the contact angle of the solution with the solid surface (assumed to be zero), and $\delta$ is the thickness of the adsorbed film of water on the solid. For a pressure of $P \approx$ -30 MPa, we estimate $r_m \approx 4.8$ nm from the first equality in Eq. (39) and, using the data of Badmann et al. [31] for $\delta$, we find $r_p \approx 5.4$ nm. Thus, only the smaller gel pores would be saturated at the point when hydration stops. For such small pores, one might question whether it is appropriate to use bulk thermodynamics to predict the equilibrium state. However, it has been demonstrated [32] that, for menisci with radii ≥ 5 nm,[2] the vapor pressure of water is accurately related to the curvature of the meniscus by the Kelvin–Laplace equation, obtained from Eqs. (32) and (39):

$$-\frac{2\gamma_{LV}\ cos(\theta)}{r_p - \delta} = \frac{RT}{\overline{V}_H} \ln(\mathrm{RH}). \tag{40}$$

Therefore, the macroscopic approach is justified in the present case. The pores that do not contain liquid water at RH = 0.8 will still contain an adsorbed film with a thickness of $\delta \approx 0.6$ nm [31]; since that film must have the same chemical potential as the liquid, it will also not react with the cement.

Of course, it is not always possible to arrest a hydration reaction by lowering the RH. For example, for the hydration of calcium oxide,

$$CaO + H_2O \rightarrow Ca(OH)_2 \tag{41}$$

the equilibrium constant is [33]

$$K_{C \leftrightarrow CH} = \frac{a_{CH}}{a_C a_H} = \frac{1}{a_H} \doteq 10^{10.02}. \tag{42}$$

This indicates that the hydration reaction will occur for $a_H > 9.5 \times 10^{-11}$ at atmospheric pressure. Since the solubility of CH is low, the activity of the solution is near unity, so the reaction will go to completion. The net volume change from this reaction is −1.72 $cm^3$/g, since the molar volume of the oxide is $\overline{V}_C = 16.79$ $cm^3$/mole; therefore, a negative pressure will inhibit the reaction. Proceeding as above, we find that the relative humidity needed to stop reaction (41) is absurdly small: $\mathrm{RH} = 1.2 \times 10^{-105}$. The lowest RH that liquid water can sustain without cavitation is about 0.4 [34], so this reaction will always proceed. The reason why negative pressure can arrest the hydration of $C_3S$, but not the hydration of CaO, is the difference of 27 orders of magnitude in the equilibrium constants for the two materials. If we allow for a change in mechanism in the dissolution of CaO, as has been suggested to occur for $C_3S$ [20], then the RH needed to stop hydration is larger, but still not physically realizable, as shown in Appendix 2.

## 8. Conclusions

These simple thermodynamic arguments indicate that the stopping of hydration often reported to occur below 80% can be explained quantitatively on the basis of the change in water activity. The

[2] In the experiments by Fisher and Israelachvili, the meniscus resembles a groove around the perimeter of a disk whose radius ($R$) is large compared to its thickness (~2 $r_m$), so the curvature is $1/R + 1/r_m \approx 1/r_m$. Since the meniscus is approximately cylindrical, $r_m \approx 5$ nm when RH ≈ 0.9; for a hemispherical meniscus, that radius corresponds to RH ≈ 0.8.

decrease in activity is caused primarily by the negative capillary pressure, not by the solute, which is at millimolar concentrations, owing to the low solubilities of the solid products. The calculation is sensitive to the molar volumes of the solids, so the quality of the prediction depends on the validity of our estimates, which are based on measured volumes of related compounds. The results also depend on the solubility products, some of which are controversial.

## Appendix 1. Influence of non-hydrostatic stress

Based on an analysis by Gibbs [35], Sekerka and Cahn [25] show that the molar free energy difference, $\Delta G$, between a solid in a non-hydrostatic versus a hydrostatic state of stress is

$$\Delta G = \frac{q_1^2 - 2\nu q_1 q_2 + q_2^2}{2E/V_m} \tag{43}$$

where $E$ and $\nu$ are, respectively, Young's modulus and Poisson's ratio for the solid, $V_m$ is its molar volume, and $q_k = \sigma_3 - \sigma_k$ (with $k = 1$ or 2), where the $\sigma_k$ are the principal stresses; the stress normal to the surface in contact with the liquid is $\sigma_3 = -(P - P_0)$ and is not equal to the other two stress components. To evaluate this result, we make use of the mean pressure on the solid phase, which is defined as

$$P_S - P_0 = -\frac{\sigma_1 + \sigma_2 + \sigma_3}{3}. \tag{44}$$

From Eqs. (12) and (13) of Ref. [36], the mean pressure in the solid phase of the paste is

$$P_S - P_0 = -\frac{\phi\,(P - P_0)}{1 - \phi} \tag{45}$$

where $\phi$ is the porosity or volume fraction of liquid in the system. (In Ref. [36], $P_0$ was neglected.) If we assume that $\sigma_1 \approx \sigma_2$, then Eqs. (44) and (45) lead to

$$\sigma_1 = \sigma_2 = \frac{(P - P_0)\,(1 + 2\phi)}{2\,(1 - \phi)}. \tag{46}$$

Using this result in Eq. (43),we find

$$\Delta G = \frac{V_m\,(1-\nu)\,q_1^2}{E} = \frac{V_m\,(1-\nu)}{E}\left(\frac{3(P - P_0)}{2(1-\phi)}\right)^2. \tag{47}$$

To appreciate the magnitude of this effect we can compare it to the chemical potential change from the reaction, expressed in Eq. (10).We can ask, what pressure difference, $\Delta P$, would have to be applied to the liquid to produce a change in $\Delta\mu$ comparable to that in Eq. (47)? The result is

$$\Delta P = \frac{\Delta G}{\Delta \overline{V}} = \frac{V_m\,(1-\nu)}{\Delta \overline{V}\,E}\left(\frac{3(P - P_0)}{2(1-\phi)}\right)^2. \tag{48}$$

It is obvious that this will be small, owing to the presence of the factor of $(P - P_0)/E$. Using the molar volumes given in the text, along with $E = 135$ GPa and $\nu = 0.3$ [37], and $\phi \approx 0.3$, we find that $\Delta P \approx -2.9 \times 10^{-4}$ MPa for reaction II, and $-4.2 \times 10^{-4}$ MPa for reaction I. Therefore, the error resulting from treating the solid as if it were under a hydrostatic stress equal to $-P$ is negligible.

## Appendix 2. Change in dissolution mechanism of CaO

The extremely low relative humidity needed to stop the hydration of CaO contrasts strongly with the one found for $C_3S$. The main reason for this lies in the fact that we have used an equilibrium constant for $C_3S$ that is believed to represent the solubility of the surface of this mineral after it has come into contact with water. We are not aware of corresponding data for CaO. We may however attempt to estimate such a change in reactivity by another means. To do this we use an argument based on the undersaturation of CaO given as:

$$\sigma = \ln\left(\frac{Q_C}{K_C}\right) \tag{49}$$

where the equilibrium constant for dissolution of CaO is [15] $K_C = 10^{4.59}$. Following notions developed in geochemistry, although for less soluble minerals, it is assumed that dissolution substantially decreases if this undersaturation (in absolute terms) decreases below a critical value denoted $\sigma_{crit}$. As values of undersaturation are negative, this means that the reaction will slow down if $\sigma > \sigma_{crit}$. As before, we assume that the system is in equilibrium with calcium hydroxide, so

$$Q_C = \frac{K_{CH}}{a_H} \tag{50}$$

where $K_{CH}$ is the equilibrium constant for dissolution of CH ($6.4 \times 10^{-6}$), so that Eq. (49) can be written as

$$\sigma = \ln\left(\frac{K_{CH}}{a_H K_C}\right) > \sigma_{crit} \tag{51}$$

which means that

$$a_H < \left(\frac{K_{CH}}{K_C}\right) exp(-\sigma_{crit}). \tag{52}$$

The critical undersaturation below which etch pits cannot be spontaneously nucleated [38] is

$$\sigma_{crit} = -\frac{2\pi^2\gamma^2\Omega}{RTSb^2\alpha} \tag{53}$$

where $\gamma$ is the solid–liquid interfacial energy, $\Omega$ is the molar volume (16.7 $cm^3$/mol), $S$ is the shear modulus (74 GPa), $b$ is the Burger vector (0.3 nm) and $\alpha$ is a parameter equal to 1 for screw dislocations and to $1 - \nu$ for clean edges, where $\nu$ is Poisson's ratio (0.22) [39].

We conclude that the reaction rate would drastically reduce if the water activity satisfies the following condition:

$$a_H < \left(\frac{K_{CH}}{K_C}\right) \exp\left(\frac{2\pi^2\gamma^2\Omega}{RTSb^2\alpha}\right). \tag{54}$$

To apply this expression quantitatively, the only missing parameter is the solid–liquid interfacial energy. For Ca $(OH)_2$, experimental values of $\gamma \approx 65$ mJ/$m^2$ have been reported [40]. For CaO, we use [41] $\gamma \approx 200$ mJ/$m^2$ and $\alpha = 1$, and obtain a critical relative humidity of $\sim 3.7 \times 10^{-10}$, which is only about a factor of 4 larger than the value we obtained earlier. This is a preliminary estimate of $\gamma$ from a molecular dynamics simulation, following an approach that has been successful for gypsum [42]. The same approach predicts that the solid–vapor interfacial energy of CaO is ~1000 mJ/$m^2$, which is close to a previous theoretical estimate [43] of 1032 mJ/$m^2$ and an experimental value [44] of $1300 \pm 200$ mJ/$m^2$. The predicted RH increases sharply with the interfacial energy, but even assuming $\gamma \approx 1000$ mJ/$m^2$ yields a critical relative humidity of about 10%. Thus, our previous conclusion stands: reduced relative humidity will not arrest the hydration of CaO. Clearly, since there is no liquid water present at such low RH, capillary pressure cannot stop hydration of CaO. Of course, the formalism we have used assumes that the solid is in contact with liquid, so the predictions of extremely low RH cannot be quantitatively accurate; nevertheless, the analysis demonstrates that there is no RH where liquid *is* present that would arrest the hydration of CaO.

## References


[1] T.C. Powers, A discussion of cement hydration in relation to the curing of concrete, Proc. Highw. Res. Board 27 (1947) 178–188.
[2] L.E. Copeland, R.H. Bragg, Self desiccation in portland cement pastes, ASTM Bull. 24 (February 1955) 34–35.
[3] L.J. Parrott, Load-induced dimensional changes of hardened cement paste, PhD Dissertation, University of London, 1973.
[4] R.G. Patel, D.C. Killoh, L.J. Parrott, W.A. Gutteridge, Influence of curing at different relative humidities upon compound reactions and porosity in Portland cement paste, Mater. Struct. 21 (1988) 192–197.
[5] V. Baroghel-Bouny, P. Mounanga, A. Khelidj, A. Loukili, N. Rafai, Autogenous deformations of cement pastes Part II. W/C effects, micro–macro correlations, and threshold values, Cem. Concr. Res. 36 (2006) 123–136.
[6] O.M. Jensen, P.F. Hansen, E.E. Lachowski, F.P. Glasser, Clinker mineral hydration at reduced relative humidities, Cem. Concr. Res. 29 (1999) 1505–1512.
[7] O.M. Jensen, Thermodynamic limit of self-desiccation, Cem. Concr. Res. 25 (1995) 157–164.
[8] P. Barret, D. Ménétrier, Filter dissolution of $C_3S$ as a function of the lime concentration in a limited amount of lime water, Cem. Concr. Res. 10 (1980) 521–534.
[9] P. Barret, D. Ménétrier, D. Bertrandie, Mechanism of $C_3S$ dissolution and problem of the congruency in the very initial period and later on, Cem. Concr. Res. 13 (1983) 728–738.
[10] D. Damidot, A. Nonat, $C_3S$ hydration in dilute and stirred suspensions: (I) study of the two kinetic steps, Adv. Cem. Res. 6 (21) (1994) 27–35.
[11] H.N. Stein, Thermodynamic considerations on the hydration mechanisms of $Ca_3SiO_5$ and $Ca_3Al_2O_6$, Cem. Concr. Res. 2 (1972) 167–177.
[12] H.M. Jennings, P.L. Pratt, An experimental argument for the existence of a protective membrane surrounding Portland cement during the induction period, Cem. Concr. Res. 10 (1979) 501–506.
[13] J.W. Bullard, R.J. Flatt, New insights into the effect of calcium hydroxide precipitation on the kinetics of tricalcium silicate hydration, J. Am. Ceram. Soc. 93 (7) (2010) 1894–1903.
[14] J.W. Bullard, A determination of hydration mechanisms for tricalcium silicate using a kinetic cellular automaton model, J. Am. Ceram. Soc. 90 (10) (2008) 2088–2097.
[15] W. Hummel, U. Berner, E. Curti, F.J. Pearson, T. Thoenen, Nagra/PSI chemical thermodynamic data base 01/01, Universal Publishers, Parkland FL, 2002.
[16] I. Lambert, H.L. Clever (Eds.), Alkaline earth hydroxides in water and aqueous solutions (solubility data series), International Union of Pure and Applied Chemistry, Oxford, England, 1992.
[17] S. Garrault-Gauffinet, A. Nonat, Experimental investigation of calcium silicate hydrate (C–S–H) nucleation, J. Cryst. Growth 200 (1999) 565–574.
[18] H.M. Jennings, Aqueous solubility relationships for two types of calcium silicate hydrate, J. Am. Ceram. Soc. 69 (8) (1986) 614–618.
[19] A. Lasaga, A. Luttge, Variation of crystal dissolution rate based on a dissolution step wave model, Science 291 (2001) 2400–2404.
[20] P. Juilland, E. Gallucci, R.J. Flatt, K. Scrivener, Dissolution theory applied to the induction period in alite hydration, Cem. Concr. Res. 40 (6) (2010) 831–844.
[21] D. Damidot, F. Bellman, B. Möser, T. Sovoidnich, Modelling the effect of electrolytes on the rate of early hydration of tricalcium silicate, in: W. Sun, K. van Breugel, C. Miao, G. Ye, H. Chen (Eds.), *First International Conference on Microstructure Related Durability of Cementitious Composites*, RILEM Proceedings PRO 61, Nanjing, China, 2008.
[22] J.W. Bullard, E. Enjolras, W.L. George, S.G. Satterfield, J.E. Terrill, A parallel reaction-transport model applied to cement hydration and microstructure development, Model. Simul. Mater. Sci. Eng. 18 (2010) 025007.
[23] D.P. Bentz, P. Lura, J.W. Roberts, Mixture proportioning for internal curing, Concr. Int. (February 2005) 35–40.
[24] E.M. Gartner, H.M. Jennings, Thermodynamics of calcium silicate hydrates and their solutions, J. Am. Ceram. Soc. 70 (10) (1987) 743–749.
[25] R.F. Sekerka, J.W. Cahn, Solid–liquid equilibrium for non-hydrostatic stress, Acta Mater. 52 (2004) 1663–1668.
[26] M.S. Paterson, Nonhydrostatic thermodynamics and its geologic applications, Rev. Geophysics Space Phys. 11 (2) (1973) 355–389.
[27] J. Bisschop, Does applied stress affect Portland cement hydration? Submitted to 13th Int. Cong. Chem. Cement, Madrid, July 3–8, 2011.
[28] Crystallographic and Crystallochemical Database for Minerals and their Structural Analogues, Institute of Experimental Mineralogy, Russian Academy of Sciences, http://database.iem.ac.ru/mincryst/s_carta.php?TOBERMORITE+4800.
[29] Crystallographic and Crystallochemical Database for Minerals and their Structural Analogues, Institute of Experimental Mineralogy, Russian Academy of Sciences, http://database.iem.ac.ru/mincryst/s_carta.php?JENNITE+7193.
[30] H.M. Jennings, A model for the microstructure of calcium silicate hydrate in cement paste, Cem. Concr. Res. 30 (2000) 101–116.
[31] R. Badmann, N. Stockhausen, M.J. Setzer, The statistical thickness and the chemical potential of adsorbed water films, J. Colloid Interface Sci. 82 (2) (1981) 534–542.
[32] L.R. Fisher, J.N. Israelachvili, Direct measurement of the effect of meniscus forces on adhesion: a study of the applicability of macroscopic thermodynamics to microscopic liquid interfaces, Colloids Surf. 3 (1981) 303–319.
[33] D.L. Parkhurst, C.A.J. Appelo, User's Guide to PHREEQC (version 2) — a computer program for speciation, batch-reaction, one-dimensional transport, and inverse geochemical calculations, water-resources investigations, Report 99–459, U.S. Geological Survey, Denver, CO, 1999.
[34] S.J. Gregg, K.S.W. Sing, Adsorption, Surface Area and Porosity, 2nd ed. Academic, London, 1982.
[35] J. Willard Gibbs, The Scientific Papers, in Two Volumes: I. Thermodynamics, Ox Bow Press, Woodbridge, CT, 1993, p. 194.
[36] G.W. Scherer, Characterization of saturated porous bodies, Concr. Sci. Eng. 37 (265) (2004) 21–30.
[37] G. Constantinides, F.-J. Ulm, The effect of two types of C–S–H on the elasticity of cement-based materials: results from nanoindentation and micromechanical modeling, Cem. Concr. Res. 34 (2004) 67–80.
[38] K. Sangwal, Etching Cryst., 15, North-Holland, 1987.
[39] U. Rössler (Ed.), Substance: calcium oxide (CaO) property: Young's, shear and bulk modulus, Poisson's ratio, Subvolume B: II–VI and I–VII Compounds, Semi-magnetic compounds, Springer, 1999.
[40] D.H. Klein, M.D. Smith, Homogeneous nucleation of calcium hydroxide, Talanta 15 (1968) 229–231.
[41] R.K. Mishra and H. Heinz, Univ. Akron, personal communication.
[42] R.K. Mishra, R.J. Flatt, H. Heinz, Molecular understanding of directional surface and interface tensions of gypsum and calcium sulfate hemihydrate, Submitted to 13th Int. Cong. Chem. Cement, Madrid, July 3-8, 2011.
[43] J.E. Lennard-Jones, P.A. Taylor, Some theoretical calculations of the physical properties of certain crystals, Proc. Roy. Soc. A 109 (1925) 476–508.
[44] S. Brunauer, D.L. Kantro, C.H. Weise, The surface energies of calcium oxide and calcium hydroxide, Can. J. Chem. 34 (1956) 729–742.